Available online at www.sciencedirect.com
SCIENCE DIRECT®
Journal of Nuclear Materials 343 (2005) 333–340
journal of nuclear materials
www.elsevier.com/locate/jnucmat

Comparison of the corrosion behavior of austenitic and ferritic/martensitic steels exposed to static liquid Pb–Bi at 450 and 550 °C

Y. Kurata *, M. Futakawa, S. Saito

Center for High Intensity Proton Accelerator Facilities, Japan Atomic Energy Research Institute, Tokai-mura, Ibaraki-ken 319-1195, Japan

Abstract

Static corrosion tests of various steels were conducted in oxygen-saturated liquid Pb–Bi eutectic at 450 °C and 550 °C for 3000 h to study the effects of temperature and alloying elements on corrosion behavior in liquid Pb–Bi. Corrosion depth decreases at 450 °C with increasing Cr content in steels regardless of ferritic/martensitic steels or austenitic steels. Appreciable dissolution of Ni and Cr does not occur in the three austenitic steels at 450 °C. Corrosion depth of ferritic/martensitic steels also decreases at 550 °C with increasing Cr content in steels whereas corrosion depth of austenitic steels, JPCA and 316SS becomes larger due to ferritization caused by dissolution of Ni at 550 °C than that of ferritic/martensitic steels. An austenitic stainless steel containing about 5%Si exhibits fine corrosion resistance at 550 °C because the protective Si oxide film is formed and prevents dissolution of Ni and Cr.

PACS: 28.41.T; 81.65.K

1. Introduction

High flux neutrons produced by spallation reaction between high energy protons and heavy metals can bring about various possibilities in the field of science and technology [1,2]. Accelerator Driven Systems (ADSs) have been proposed for the purpose of treatment of nuclear wastes [3,4]. The ADSs consist of a proton accelerator, a spallation target and subcritical core. Liquid Pb–Bi eutectic is a potential candidate of the target and coolant. Since the solubility of main elements of structural materials is high in liquid Pb–Bi [5,6], the liquid metal has corrosive properties. Therefore, corrosion tests of the structural materials in liquid Pb–Bi have been actively performed recently [7–16]. The long-term study on reactors using liquid Pb alloys as a coolant has been conducted in Russia and technologies and knowledge on liquid Pb alloys have been accumulated [5,7,8]. Recently experiments have been conducted using new Pb–Bi loops and corrosion test apparatuses fabricated on the basis of knowledge obtained in Russia.

In previous Russian studies [5,7,8], importance of oxygen control in liquid Pb–Bi was pointed out and martensitic steels containing Si were developed for corrosion resistance. From the viewpoints of material corrosion it is important to know what kind of corrosion

* Corresponding author. Tel.: +81 29 282 5059; fax: +81 29 282 6489.
E-mail address: ykurata@popsvr.tokai.jaeri.go.jp (Y. Kurata).

0022-3115/$ - see front matter © 2005 Elsevier B.V. All rights reserved.
doi:10.1016/j.jnucmat.2004.07.064

phenomenon occurs in liquid Pb–Bi. Phenomena such as mass transfer, erosion, oxidation, dissolution, precipitation, grain boundary corrosion and penetration of Pb–Bi into steels occur in liquid Pb–Bi. Furthermore, the phenomenon of ferritization of the austenitic steels owing to Ni dissolution was reported [11,16].

Corrosion tests using liquid Pb–Bi loop are conducted to study flow effect, erosion and mass transfer caused by dissolution at high temperature parts and precipitation at low temperature parts. Phenomena such as oxidation, dissolution, grain boundary corrosion, penetration of Pb–Bi and ferritization can be also investigated in static corrosion tests whose purposes are understanding of basic corrosion mechanism and screening of materials. It is essential to make a corrosion map in liquid Pb–Bi in order to understand the corrosion behavior and use the liquid metal as target and coolant of ADSs. Parameters for the corrosion map are temperature, temperature gradient at high temperature parts and low temperature parts, alloying elements in steels, oxygen concentration in liquid Pb–Bi, flow velocity, irradiation, etc. Equipments and the first R&D program for the corrosion map are described in Ref. [12].

In this study, effects of temperature and contents of alloying elements, Cr, Ni and Si in steels on corrosion behavior are investigated using a static corrosion apparatus for the purpose of drawing the corrosion map. Then corrosion resistant steel in liquid Pb–Bi is proposed through this study.

2. Experimental

2.1. Specimens

Table 1 shows chemical compositions of materials used in the experiment. F82H, Mod.9Cr–1Mo steel, 410SS, 430SS and 2.25Cr–1Mo steel are ferritic/martensitic steels. The 14Cr–16Ni–2Mo steel (JPCA), 316SS and SX (Trademark of the Sandvik Corporation) are austenitic stainless steels. The SX steel is an alloy developed for use in a sulfuric acid environment and the characteristic of the steel is high Si content. The size of corrosion specimens was 15 mm × 30 mm × 2 mm, and a hole of 7.2 mm diameter for installation was made at the top of the specimen. Corrosion specimens were polished using emery papers up to #600.

2.2. Corrosion test apparatus and procedure

The static corrosion test apparatus in liquid Pb–Bi was described in detail elsewhere [12]. Components contacting liquid Pb–Bi were made of quartz in the corrosion equipment. As received eutectic Pb–Bi (45Pb–55Bi) of 7 kg was used in the present test. The chemical composition of the Pb–Bi was the following: 55.60Bi–0.0009Sb–0.0002Cu–0.0001Zn–0.0005Fe–0.0007As–0.0005Cd–0.0001Sn–Bal.Pb (wt%). The Pb–Bi was melted in a pot under Ar gas environment. Ar gas of 99.9999% purity was used as a cover gas over the liquid Pb–Bi. Corrosion tests were conducted at 450 °C and 550 °C for 3000 h. PbO was formed on the surface of the liquid Pb–Bi and corrosion tests were made in oxygen-saturated liquid Pb–Bi. Oxygen saturation concentration was estimated to be 3.2×10^{-4} wt% at 450 °C and 1.2×10^{-3} wt% at 550 °C using the equation in the literature [5].

Test specimens were cleaned in silicone oil at about 170 °C after the corrosion tests to remove Pb–Bi stuck to the surface of the specimens. However, there was adherent Pb–Bi left on some parts of the specimen surface. Analyses were made using an optical microscope, a scanning electron microscope (SEM) with energy dispersion X-ray (EDX) for the specimen plated with copper to protect corrosion films during polishing. X-ray diffraction was also used to characterize corrosion products.

3. Experimental results

Figs. 1 and 2 show optical micrograhs of the cross-sections of specimens after corrosion in liquid Pb–Bi for 3000 h at 450 °C and 550 °C, respectively. Grey corrosion films are observed under copper plating. The

Table 1
Chemical composition of materials tested in the static corrosion experiment (mass%)

	C	Si	Mn	Cr	Ni	Mo	Fe	V	N	W	Ti	Al	Cu
F82H	0.095	0.10	0.01	7.72	<0.02	<0.01	Balance	0.18	0.010	1.95	0.005	<0.001	–
Mod.9Cr–1Mo steel	0.10	0.30	0.40	8.41	0.06	0.88	Balance	0.20	0.047	<0.0005	<0.01	0.033	–
14Cr–16Ni–2Mo (JPCA)	0.058	0.50	1.54	14.14	15.87	2.29	Balance	0.03	0.003	0.010	0.22	0.012	–
410SS	0.067	0.31	0.80	12.21	0.12	0.02	Balance	0.07	0.013	–	<0.01	0.002	–
430SS	0.080	0.52	0.23	16.24	0.15	0.02	Balance	0.10	0.024	–	<0.01	0.007	–
2.25Cr–1Mo steel	0.10	0.34	0.44	2.18	0.02	0.92	Balance	0.01	0.009	–	<0.01	0.002	–
Fe	0.002	–	–	–	–	–	Balance	–	0.001	–	–	–	–
316SS	0.04	0.69	1.22	16.83	10.79	2.06	Balance	–	–	–	–	–	–
SX	0.010	4.80	0.60	17.58	19.08	0.356	Balance	–	–	–	–	–	2.14

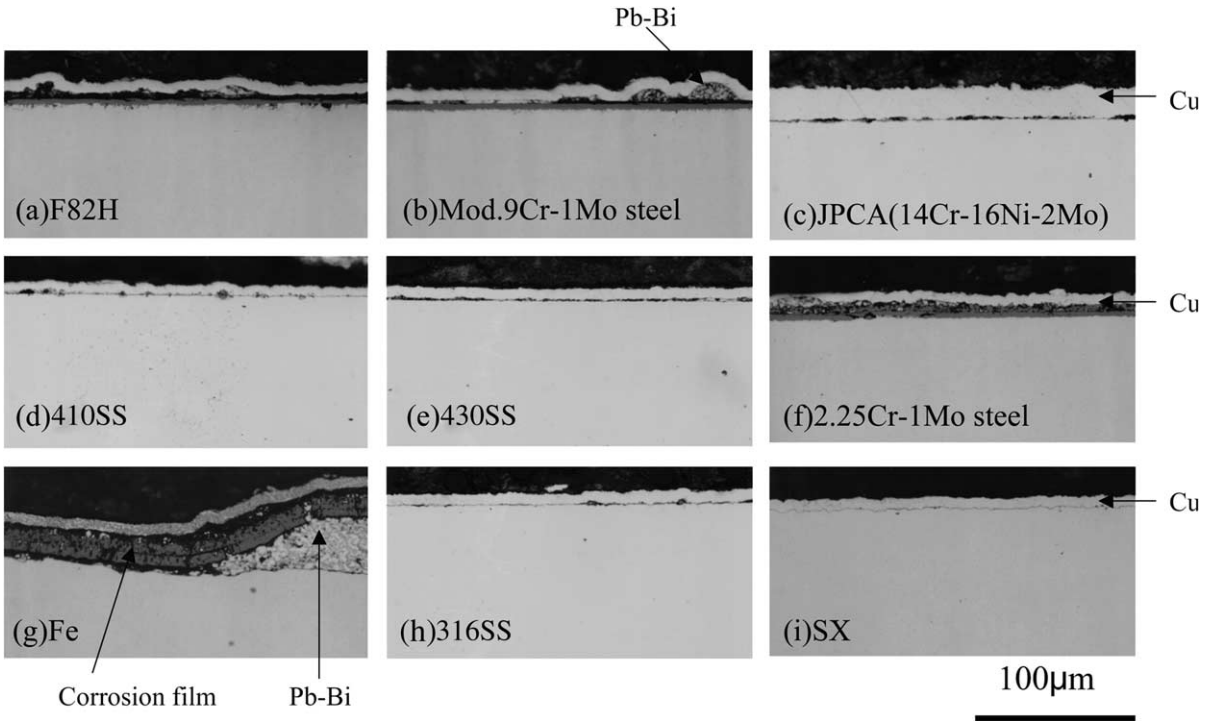

Fig. 1. Optical micrographs of cross-sections of (a) F82H, (b) Mod.9Cr–1Mo steel, (c) JPCA, (d) 410SS, (e) 430SS, (f) 2.25Cr–1Mo steel, (g) Fe, (h) 316SS and (i) SX after corrosion in liquid Pb–Bi at 450 °C.

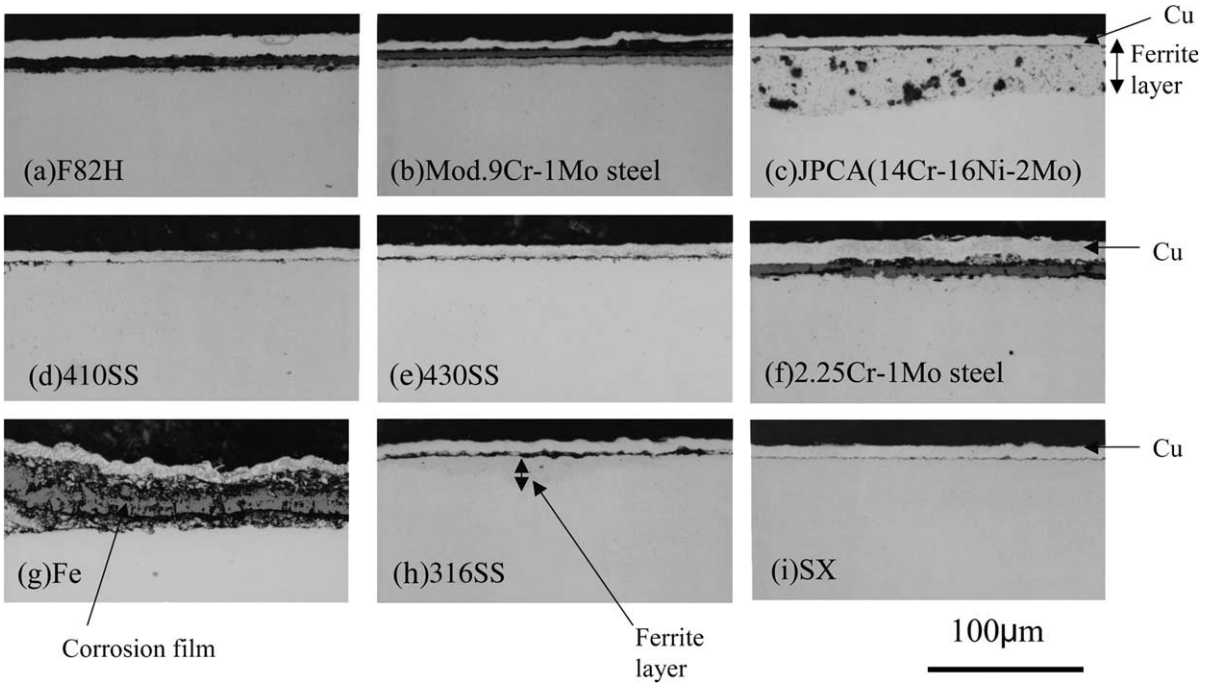

Fig. 2. Optical micrographs of cross-sections of (a) F82H, (b) Mod.9Cr–1Mo steel, (c) JPCA, (d) 410SS, (e) 430SS, (f) 2.25Cr–1Mo steel, (g) Fe, (h) 316SS and (i) SX after corrosion in liquid Pb–Bi at 550 °C.

adherent Pb–Bi left on some parts of the specimen surface is also recognized, for example, in Fig. 1(b). Curving and peeling of corrosion films are observed in Fe whose corrosion films are thick as shown in Fig. 1(g) and Fig. 2(g). There is a ferrite layer mentioned later near the surface region of JPCA and 316SS after corrosion at 550 °C for 3000 h in Fig. 2(c) and (h). Formation of the ferrite layer was not observed in the specimens after corrosion at 450 °C and in the SX specimen after corrosion at 550 °C. Furthermore, the grain boundary corrosion was observed in F82H, Mod.9Cr–1Mo steel, 410SS, 430SS and 2.25Cr–1Mo steel as shown typically for 2.25Cr–1Mo steel in Fig. 3.

The results for EDX analysis of Mod.9Cr–1Mo steel after corrosion at 450 °C are shown in Fig. 4. It is found that the corrosion film is oxide of Fe and Cr from the elements mapping. Fig. 4 shows that double layer oxides are formed: the outer corrosion film is a fragile iron oxide and the inner corrosion film is Cr–Fe spinel. This result agrees with the result that outer magnetite and inner Cr–Fe spinel were formed during corrosion in liquid Pb–Bi [12,15]. Fig. 5 shows the result of line analysis for 2.25Cr–1Mo steel after corrosion in liquid Pb–Bi at 450 °C for 3000 h. The outer corrosion film of iron oxide is porous and fragile because Pb and Bi penetrate into the outer magnetite and reach the Cr–Fe spinel surface.

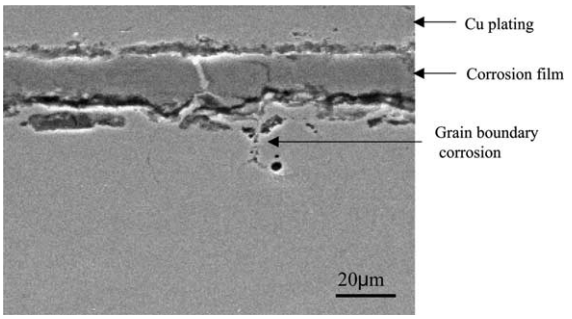

Fig. 3. SEM image of cross-section of 2.25Cr–1Mo steel after corrosion in liquid Pb–Bi at 550 °C for 3000 h.

The corrosion films are thin in steels of JPCA, 410SS, 430SS, 316SS and SX containing Cr more than 12% as shown in Figs. 1 and 2. The corrosion films of the steels except for SX are oxides of Fe and Cr. Fig. 6 shows the results of EDX analysis for JPCA specimen after corrosion at 450 °C. No decrease in Cr, Ni and Fe concentrations near the surface region means no appreciable dissolution of these elements into liquid Pb–Bi. On the other hand, Fig. 7 shows the formation of the layer with excessive decrease in Ni and Cr under the corrosion film for JPCA specimen at 550 °C. Enrichment of O, Cr and Fe is observed in the corrosion film. Furthermore, Pb and Bi penetrate into the layer.

Figs. 8 and 9 show the results of X-ray diffraction of JPCA and SX specimens before and after corrosion at 550 °C, respectively. It is found that the layer with excessive decrease in Ni and Cr is a ferrite phase because peaks of Fe–Cr ferrite phase(α) with bcc structure are detected on JPCA specimen after corrosion at 550 °C as shown in Fig. 8. On the other hand, only peaks of austenite phase(γ) are detected on SX specimen even after corrosion at 550 °C in Fig. 9. Although a very thin oxide film seems to exist on the SX specimen, the detail of the film is not clear in Fig. 2. Fig. 10 shows the result of EDX line analysis made with higher magnification. A thin continuous film with the thickness of 200–400 nm is formed on the surface of the SX specimen. The film is an oxide composed of Si and O. Enrichment of Cr, Fe and Ni cannot be observed in the oxide film. It is found from the comparison of corrosion behavior between JPCA

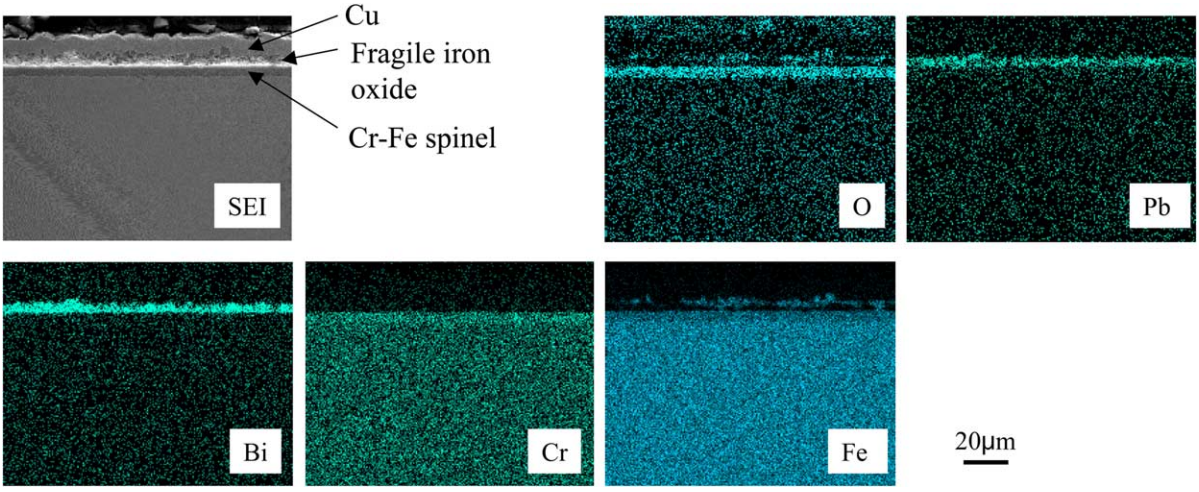

Fig. 4. EDX analysis of the cross-section of Mod.9Cr–1Mo steel after corrosion in liquid Pb–Bi at 450 °C for 3000 h.

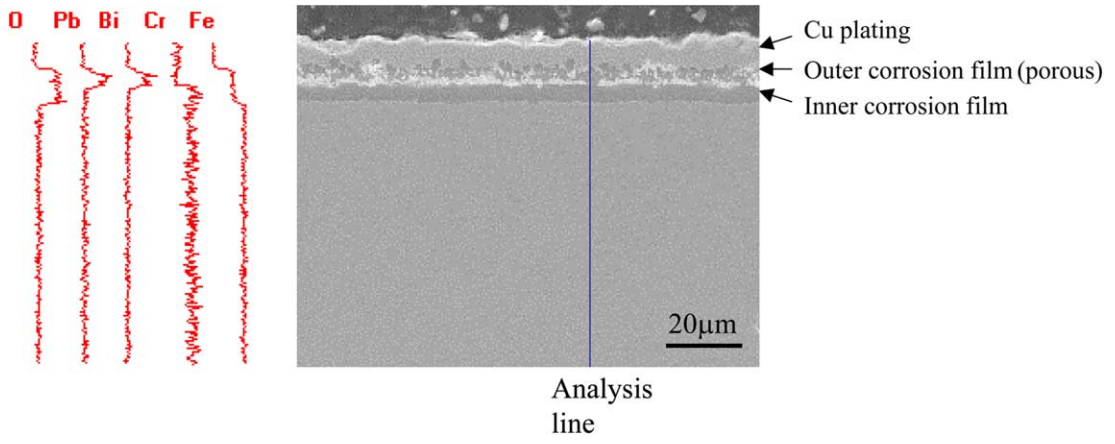

Fig. 5. Line analysis of the cross-section of 2.25Cr–1Mo steel after corrosion in liquid Pb–Bi at 450 °C for 3000 h.

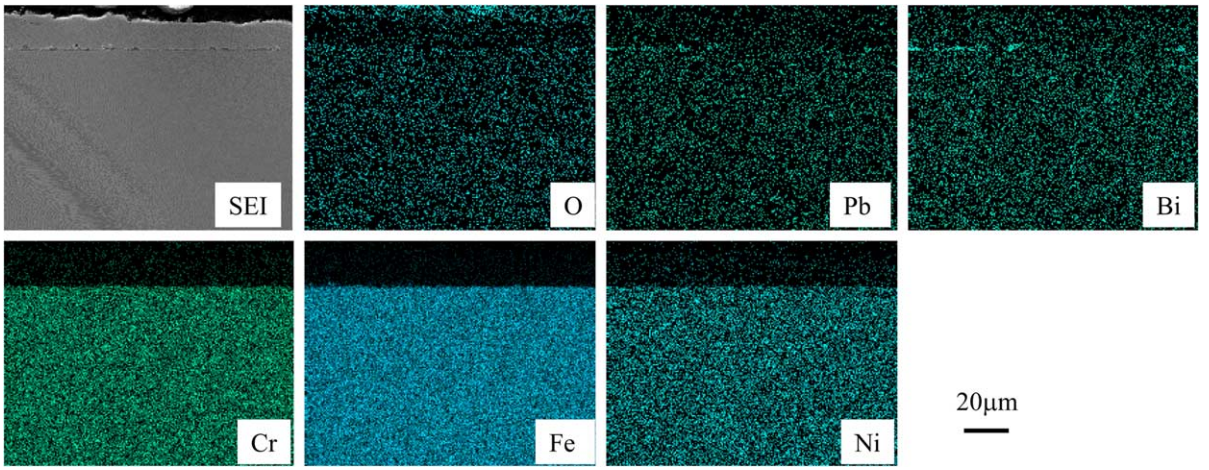

Fig. 6. EDX analysis of the cross-section of JPCA after corrosion in liquid Pb–Bi at 450 °C for 3000 h.

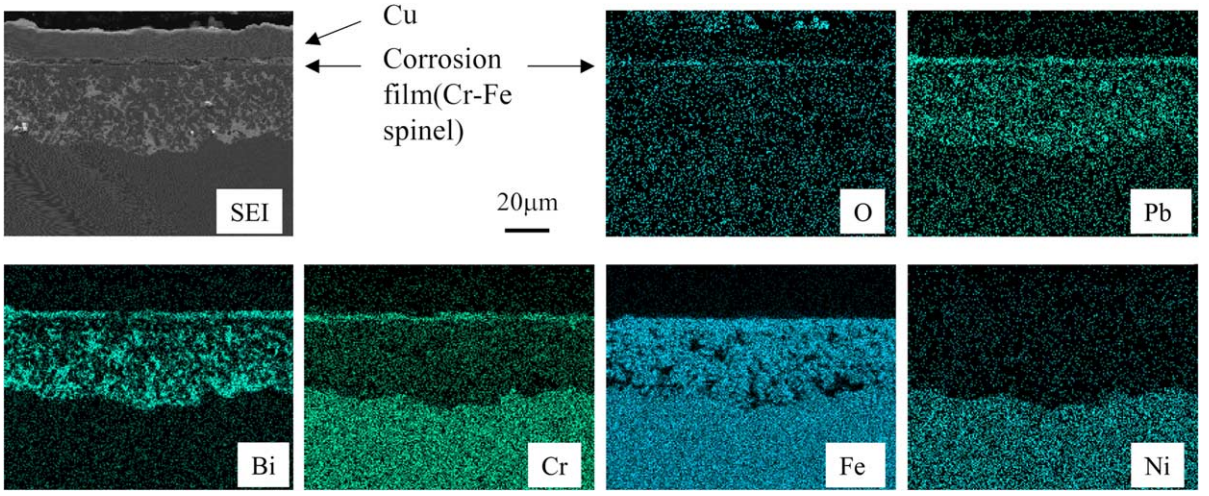

Fig. 7. EDX analysis of the cross-section of JPCA after corrosion in liquid Pb–Bi at 550 °C for 3000 h.

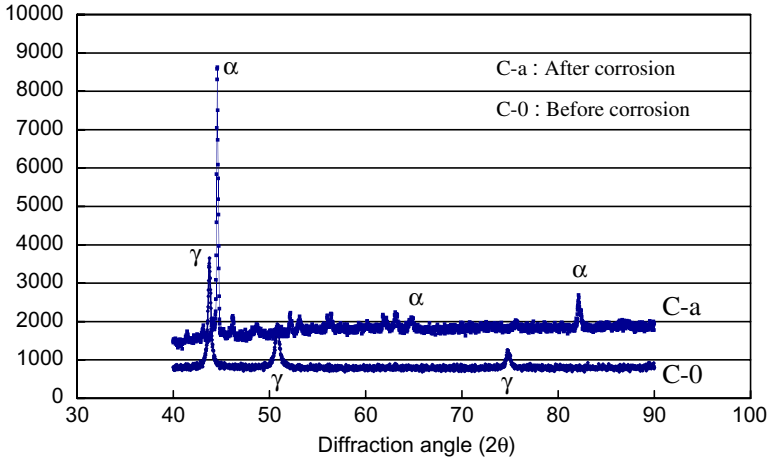

Fig. 8. X-ray diffraction spectra of JPCA before and after corrosion at 550 °C.

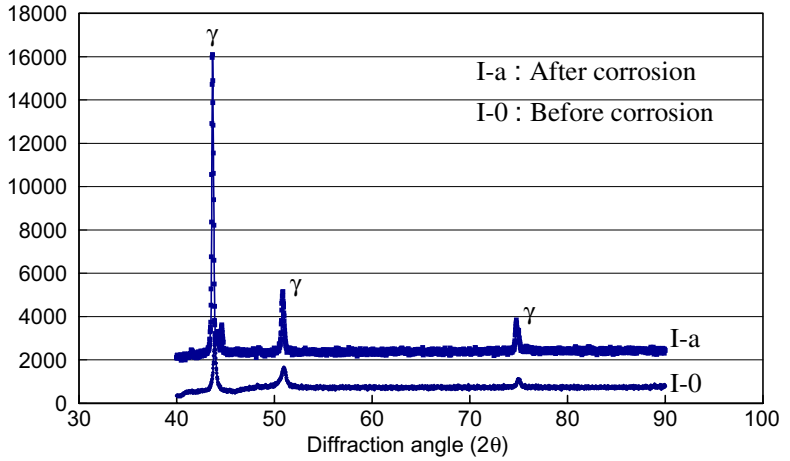

Fig. 9. X-ray diffraction spectra of SX before and after corrosion at 550 °C.

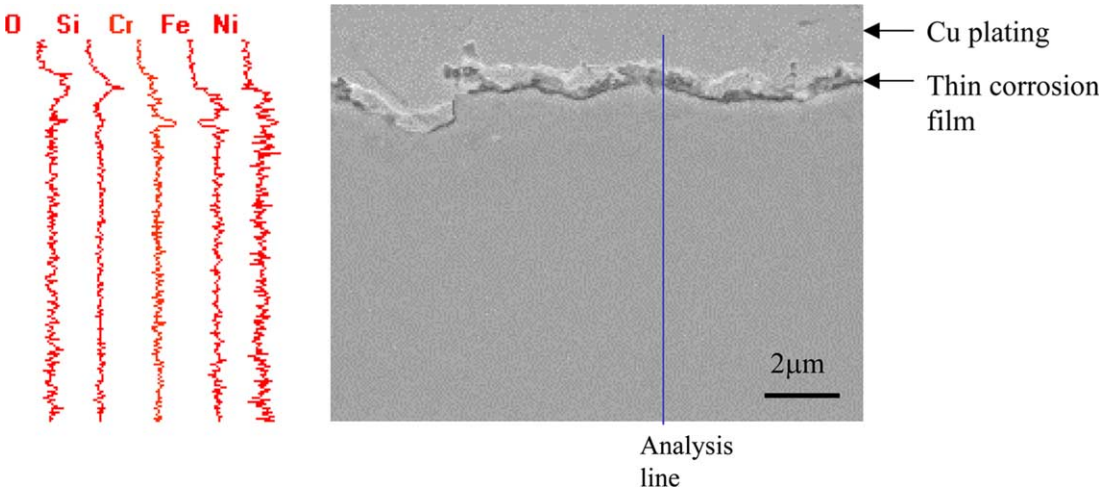

Fig. 10. Line analysis of the cross-section of SX after corrosion in liquid Pb–Bi at 550 °C for 3000 h.

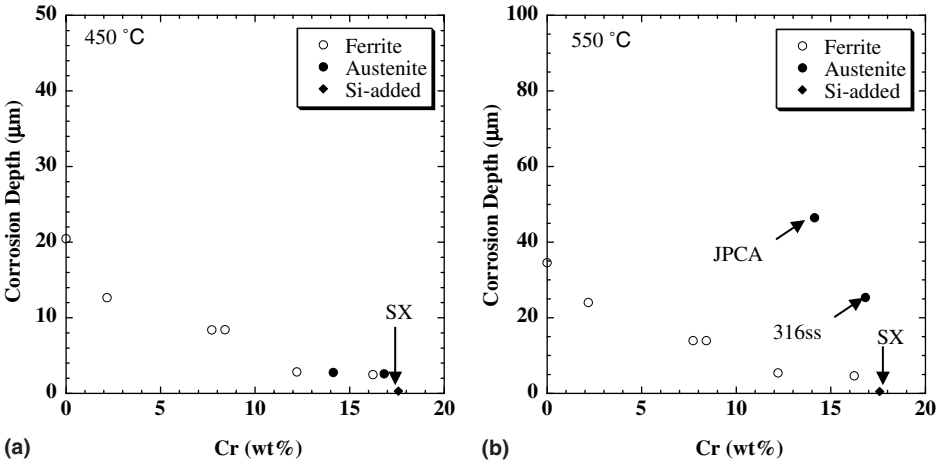

Fig. 11. Relationship between corrosion depth and Cr content in steels. The corrosion test was conducted in liquid Pb–Bi at (a) 450 °C and (b) 550 °C, respectively.

and SX that the thin oxide film on SX prevents ferritization of the austenitic steel because Ni and Cr concentrations keep constant beneath the oxide film.

The relationship between corrosion depth and Cr content in steels is shown in Fig. 11. The corrosion depth is defined as the sum of the thickness of the oxide film, the grain boundary corrosion depth and the thickness of the formed ferrite layer. Corrosion depth of steels decreases at 450 °C with increasing Cr content of the steels regardless of ferritic/martensitic steels or austenitic steels. Corrosion depth of Si-added steel, SX is very small. Corrosion depth of ferritic/martensitic steels which is shown as an open circle in Fig. 11(b) also decreases at 550 °C with increasing Cr content of the steels while corrosion depth of austenitic steels, JPCA and 316SS becomes large because of formation of the ferrite layer at 550 °C. Corrosion depth of SX is very small at 550 °C in spite of austenitic steel.

4. Discussion

One of typical examples of corrosion damage in liquid Pb–Bi is the ferritization of austenitic steels due to dissolution of Ni [11,16]. In this study, the ferritization of JPCA and 316SS occurred in the static corrosion test at 550 °C and Pb and Bi penetrated into the formed ferrite layer. Benamati et al. [11] showed that the ferritization of austenitic stainless steels, AISI 316L and Mannet II occurred during the static corrosion test under oxygen-saturated Pb–Bi condition at 550 °C. Furthermore, Mueller et al. [16] indicated that AISI 316L exhibited dissolution of Ni and penetration of Pb and Bi into the ferrite layer during a loop test at 600 °C. Since the austenitic steel did not exhibit appreciable dissolution of Ni and Cr at 450 °C in this study, the temperature where the ferritization of JPCA and 316SS occurs under oxygen-saturated Pb–Bi condition lies between 450 °C and 550 °C. On the other hand, the corrosion film of Si oxide formed on SX in Pb–Bi at 550 °C can prevent dissolution of Ni and ferritization of the austenitic stainless steel. This information is important to draw the corrosion map in liquid Pb–Bi.

It was found that Si oxide without enrichment of Cr, Fe and Ni was formed on SX during corrosion in Pb–Bi at 550 °C in this study. It was reported that Si addition to Fe–9%Cr steel produced a protective SiO_2 layer at the oxide-metal interface and brought about significant improvement of corrosion resistance in a gas environment at 575–650 °C [17]. Benemati et al. [11] also reported that Fe–Cr oxide containing 3%Si was formed in liquid Pb–Bi and kept corrosion resistance as a result of loop tests at 450 °C and 550 °C for 700 h for Russian martensitic steel, EP823 [8] containing 2%Si. The fact that thin and dense Si oxide was formed on SX in this study is a little different from the results of formation of Fe–Cr oxides containing Si. Although it is difficult to determine the chemical composition of the thin corrosion film on SX from the EDX line analysis shown in Fig. 10, the formation of Si oxide without enrichment of Cr, Fe and Ni is recognized. As shown in Figs. 4 and 5, the outer magnetite and the inner Cr–Fe spinel oxide were formed on Mod.9Cr–1Mo steel and 2.25Cr–1Mo steel. It is considered that Cr–Fe spinel oxide was formed on JPCA because enrichment of O, Cr and Fe was detected in the corrosion film shown in Fig. 7. The thin oxide film on SX is different from magnetite and Cr–Fe spinel oxide. Figs. 8 and 9 clearly show occurrence of the ferritization on the JPCA steel and prevention of the ferritization on the SX steel. From

these results it is considered that the oxide of Fe and Cr did not play an effective role as a diffusion barrier of Ni and Cr at 550 °C. However, the film of Si oxide formed on SX during corrosion at 550 °C exhibits an effective role as a diffusion barrier of Ni and Cr. In order to clarify a corrosion-resistant mechanism by Si addition and an effective range of temperature and oxygen concentration, short-term exposure tests, corrosion tests under low oxygen condition and transmission electron microscope observation of the thin corrosion film will be necessary for Si-added steels.

As shown in Fig. 11, corrosion depth of JPCA and 316SS became very large at 550 °C due to ferritization in spite of their Cr content above 14% although the corrosion resistance of the austenitic stainless steels is higher at 450 °C than that of ferritic/martensitic steels (F82H and Mo.9Cr–1Mo steel) with Cr content of 8–9%. It means that the corrosion resistance of JPCA and 316SS deteriorates at 550 °C due to ferritization.

On the other hand, SX containing 4.8%Si exhibits high corrosion resistance to liquid Pb–Bi since the protective film of Si oxide formed during exposure to Pb–Bi prevents dissolution of Ni and ferritization. In this way, it is considered that Si addition to steels is very effective for improvement of corrosion resistance in liquid Pb–Bi. However, Si is one of elements giving harmful influence on weldability and creep properties of steels. Furthermore, Si in steels may affect irradiation properties such as swelling, radiation induced segregation and embrittlement. It is necessary to evaluate the applicability of Si added steels to ADS components from the viewpoints of not only corrosion resistance in liquid Pb–Bi but also weldability and irradiation properties.

5. Conclusions

Static corrosion tests of various steels with different contents of Cr, Ni and Si were conducted in oxygen-saturated liquid Pb–Bi at 450 °C and 550 °C for 3000 h. The following conclusions are drawn:

(1) Corrosion depth at 450 °C decreases with increasing Cr content in steels regardless of ferritic/martensitic steels or austenitic steels. Appreciable dissolution of Ni and Cr does not occur in the three austenitic steels at 450 °C. Thin oxide films are formed during exposure to liquid Pb–Bi up to 3000 h.
(2) Corrosion depth of ferritic/martensitic steels at 550 °C decreases with increasing Cr content in steels. Nickel and chromium in austenitic steels, JPCA and 316SS dissolve into liquid Pb–Bi and the thick ferrite layer is formed at 550 °C in spite of formation of Fe–Cr oxide. As a result, corrosion depth of JPCA and 316SS become larger than that of ferritic/martensitic steels.
(3) A protective oxide film composed of Si and O is formed on the surface of SX containing 4.8%Si during corrosion in liquid Pb–Bi at 550 °C. The thin oxide film prevents dissolution of Ni and Cr into Pb–Bi. The Si added austenitic steel exhibits good corrosion resistance at 550 °C up to 3000 h and under static condition in liquid Pb–Bi.

References

[1] T.A. Gabriel, J.R. Haines, T.J. McManamy, J. Nucl. Mater. 318 (2003) 1.
[2] The Joint Project Team of JAERI and KEK, JAERI-Tech 99-56, 1999.
[3] C. Rubbia, J.A. Rubio, S. Buono, F. Carminati, Conceptual design of a fast neutron operated high power energy amplifier, CERN/AT/95-44(ET), September 29, 1995.
[4] T. Mukaiyama, T. Takizuka, M. Mizumoto, Y. Ikeda, T. Ogawa, A. Hasegawa, H. Takada, H. Takano, Progr. Nucl. Energy 38 (2001) 107.
[5] B.F. Gromov, Y.I. Orlov, P.N. Martynov, V.A. Gulevsky, in: Proceedings of Heavy Liquid Metal Coolants in Nuclear Technology, HLMC'98, 5–9 October 1998, Obninsk, Russia, 1999, p. 87.
[6] J .R. Weeks, Nucl. Eng. Des. 15 (1971) 363.
[7] I.V. Gorynin, G.P. Karzov, V.G. Markov, V.S. Lavrukihin, V.A. Yakovlev, in: Proceedings of Heavy Liquid Metal Coolants in Nuclear Technology, HLMC'98, 5–9 October 1998, Obninsk, Russia, 1999, p. 120.
[8] G.S. Yachmenyov, A.Ye. Rusanov, B.F. Gromov, Yu.S. Belomytsev, N.S. Skvortsov, A.P. Demishonkov, in: Proceedings of Heavy Liquid Metal Coolants in Nuclear Technology, HLMC'98, 5–9 October 1998, Obninsk, Russia, 1999, p. 133.
[9] F. Barbier, A. Rusanov, J. Nucl. Mater. 296 (2001) 231.
[10] C. Fazio, G. Benamati, C. Martini, G. Palombarini, J. Nucl. Mater. 296 (2001) 243.
[11] G. Benamti, C. Fazio, H. Piankova, A. Rusanov, J. Nucl. Mater. 301 (2002) 23.
[12] Y. Kurata, M. Futakawa, K. Kikuchi, S. Saito, T. Osugi, J. Nucl. Mater. 301 (2002) 28.
[13] K. Kukuchi, Y. Kurata, S. Saito, M. Futakawa, T. Sasa, H. Oigawa, E. Wakai, K. Miura, J. Nucl. Mater. 318 (2003) 348.
[14] G. Mueller, G. Schumacher, F. Zimmermann, J. Nucl. Mater. 278 (2000) 85.
[15] F. Barbier, G. Benamati, C. Fazio, A. Rusanov, J. Nucl. Mater. 295 (2001) 149.
[16] G. Mueller, A. Heinzel, J. Konys, G. Schumacher, A. Weisenburger, F. Zimmermann, V. Engeliko, A. Rusanov, V. Markov, J. Nucl. Mater. 301 (2002) 40.
[17] J. Robertson, M.I. Manning, Mater. Sci. Technol. 5 (1989) 741.